Information compression at the turbulent phase transition in cold-atom gases

R. Giampaoli [1,2] J. L. Figueiredo [1] J. D. Rodrigues,[1] J. A. Rodrigues [1,3] H. Terças [1] and J. T. Mendonça [1]

[1]*Instituto de Plasmas e Fusão Nuclear, Instituto Superior Técnico, Universidade de Lisboa, 1049-001 Lisbon, Portugal*
[2]*Laboratoire Kastler Brossel, Sorbonne Université, CNRS, ENS-PSL Research University, Collège de France, 75005 Paris, France*
[3]*Departamento de Física, Universidade do Algarve, Campus de Gambelas, 8005-139 Faro, Portugal*

The statistical properties of physical systems in thermal equilibrium are blatantly different from their far-from-equilibrium counterparts. In the latter, fluctuations often dominate the dynamics and might cluster in ordered patterns in the form of dissipative coherent structures. Here, we study the transition of a cold atomic cloud, driven close to a sharp electronic resonance, from a stable to a turbulent phase. From the atomic density distribution—measured using a spatially resolved pump-probe technique—we have computed the Shannon entropy on two different basis sets. Information compression, corresponding to a minimum in the Shannon entropy, has been observed at criticality, where the system fluctuations organize into high-order (low-entropy) patterns. Being independent of the representation used, this feature is a property shared by a vast class of physical systems undergoing phase transitions.

I. INTRODUCTION

The macroscopic properties of physical systems in equilibrium can be described in terms of free-energy landscapes [1,2]. Far from equilibrium, spatiotemporal dynamics are dominated by fluctuations, which get amplified and often lead to the formation of coherent dissipative structures [2–5]. Some of these phenomena can be described with a formalism analogous to the one used in equilibrium phase transitions, a striking example being the analogy of a laser threshold and a second-order phase transition [6,7]. Moreover, when phase transitions involve loss of global symmetry, the statistical properties can often be captured by a single order parameter, as in the case of stable-to-turbulence transitions [8,9]. In general, however, despite the existence of several theoretical models, when it comes to phase transitions of nonequilibrium systems, evidence of universality is still very poor [10].

In recent years, extensions of the methods used in equilibrium to far-from-equilibrium scenarios have been proposed by resorting to information theory [2,5,11,12]. The latter require a more limited set of assumptions and find applications in different fields [13]. Information (Shannon) entropy is a key quantity in the information theoretical analysis of phase transitions, playing the role of its thermodynamic counterpart. In a phase transition, the state of a system may be described by some generic field $\Phi \equiv \Phi(\mathbf{r}, t; \delta)$, where δ is the stress parameter (often, but not always, the thermodynamic temperature). Given a complete and orthogonal basis for the space of square-integrable functions, the field can be uniquely identified by the projections onto the basis elements. The link between the thermodynamic and information theories is provided by the expansion coefficients: these can be viewed both as the spectral energy content of the system (that is spread over several physical modes) and, at the same time, as the probability distribution which encodes the information of each mode [5,14]. A phase transition can then be interpreted as a change in the group symmetries of the field when the stress parameter attains some critical value δ_c. Typically, the transition mechanism can be described by a single (or few) order parameter ψ, which spontaneously breaks the symmetry at the critical point [15].

In this paper, we report the observation of information compression in the stable to turbulent phase transition in a cold-atom cloud, occurring far from equilibrium when the cooling laser frequency is set near the electronic resonance [16,17]. Measures have been performed on a cold rubidium gas by directly probing various statistically independent realizations of the atomic density distribution (the field Φ) whose statistical properties are controlled by the cooling laser detuning δ. By varying δ, the system goes from a stable-symmetric (uniform) phase to a turbulent one, where the global symmetry is lost and quasicoherent structures emerge. At criticality the system spontaneously organizes, showing both a long-range local order and the formation of oscillating global patterns. We compute the Shannon entropy on two different bases for multiple realizations of the atomic density distribution and, at the critical point, an entropy minimum—associated with information compression—is observed. Remarkably, this minimum is independent of the representation used, which points out the transition as a state of maximum organization and emerges as a potentially universal property of a large class of phase transitions. Our results provide a tool that can be easily extended to other far-from-equilibrium scenarios where a more quantitative description is desired, such as in
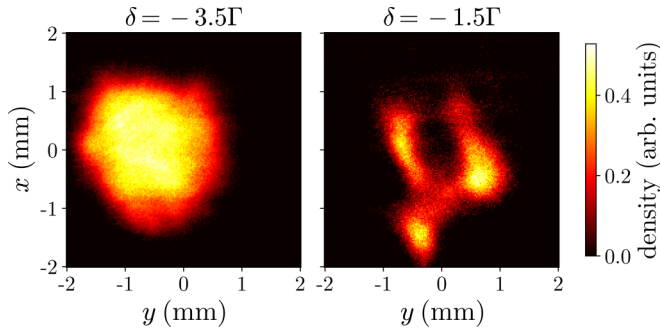
FIG. 1. Snapshots of a single realization of the atomic cloud density distribution in the stable phase ($\delta = -3.5\Gamma$) and in the turbulent phase ($\delta = -1.5\Gamma$). The cold-atom cloud in the turbulent regime is highly inhomogeneous and is characterized by strong spatiotemporal dynamics which feature the emergence of quasicoherent structures. The images have been retrieved with the spatially resolved pump-probe technique described inx Ref. [16].

the study of biological flows [18], spatiotemporal chaos [19], or growing interfaces [20].

II. TURBULENT PHASE TRANSITION IN A COLD RUBIDIUM GAS

Experiments have been performed on a magneto-optical trap (MOT) [21], where around 10^9 ^{85}Rb atoms are cooled and trapped at approximately 200 μK [22,23]. A spatially resolved pump-probe diagnostic allows direct access to the atomic density distribution along a thin section of the atomic cloud. As a result, the collected images can be safely interpreted as two-dimensional (2D) atomic density maps [16]. The experiments have been carried out by keeping the magnetic field approximately constant ($\nabla B = 10$ G/cm) and the cooling laser detuning δ ranging from -4Γ to -0.75Γ in steps of 0.25Γ, with Γ denoting the transition linewidth. For each value of δ, a total of 100 measurements have been performed, effectively probing different system realizations. Each measurement consists of a loading step, during which the atomic gas is trapped and cooled until it forms a stationary cloud, followed by the MOT unloading, after which the pump-probe sequence is executed. When the frequency of the cooling lasers is brought close to resonance, the cold-atom cloud passes through a sharp transition from a stable, spatially uniform phase to a turbulent phase [16]. Figure 1 shows the density profiles of the atomic cloud in both phases. The turbulent regime is characterized by strong spatiotemporal fluctuations which develop as the cold-atom gas is continuously cooled and trapped in the range $\delta \in [-2\Gamma, -0.75\Gamma]$. Fluctuation power data show the transition effectively taking place in the interval $\delta \in [-2.25\Gamma, -2\Gamma]$: The resolution on δ is determined by the laser linewidth, which is of the same magnitude as the minimum detuning step $\Delta\delta = 0.25\Gamma$. The stable-turbulent transition is marked by an abrupt increase in the power of density fluctuations and by a peak in the fluctuation correlation length at the transition onset $\delta = -2\Gamma$. The turbulent dynamics originate from a fluid-dynamic instability, known as photon-bubble instability [24], which stems from the strong coupling of the atomic fluid with diffusive

radiation. Photon bubbles leave a clear signature in the atomic fluctuation density in the form of quasicoherent structures.

III. INFORMATION ENTROPY

Information theory [25] provides the tools to measure the quantity of information resulting from the observation of an event. The information content I_j [26] is defined in such a way that unlikely events carry more information and it is computed as $I_j \equiv \log(1/p_j) = -\log(p_j)$, where p_j is the probability of the jth event, $\sum_j p_j = 1$. The Shannon entropy S is then defined as the average information content per event, $S[\{p_j\}] = -\sum_j p_j \log(p_j)$. The maximum entropy corresponds to a flat distribution, in which no outcome is favored: Each observation produces, on average, a high amount of information. Hence, by comparing the value of S of the actual probability distribution to its maximum value attained for a flat distribution over the same ensemble, we get a quantitative measure of information compression. Highly compressed ensembles are characterized by clustered probability distributions which result in low-entropy values.

In order to interpret critical phenomena, we apply the same information-theory description to the density field $\Phi(\mathbf{r}, t; \delta)$ by decomposing it onto its basis elements. Independently of the basis choice, the meaning of low-entropy values is the same: A low number of highly probable modes dominates the system dynamics, meaning that less information is needed to characterize the system, resulting in compression in information space. The Shannon entropy defined from the field expansion onto Fourier modes is called configurational entropy, first introduced in Ref. [27] as a measure for localized energy configurations. The configurational entropy is defined in terms of the modal fraction $f(\mathbf{k}) = P(\mathbf{k})/\sum_{\mathbf{k}} P(\mathbf{k})$ as

$$S_C = -\sum_{\mathbf{k}} f(\mathbf{k}) \log[f(\mathbf{k})], \tag{1}$$

where $P(\mathbf{k}) = \int d\mathbf{r}\, e^{-i\mathbf{k}\cdot\mathbf{r}} \langle \tilde{\Phi}(\mathbf{r})\tilde{\Phi}(0) \rangle$ is the 2D power spectrum, $\tilde{\Phi}(\mathbf{r}) = \Phi(\mathbf{r}) - \langle \Phi(\mathbf{r}) \rangle$ is the 2D atomic density fluctuation, and $\mathbf{k} = (k_x, k_y)$ the wave vector. The symbol $\langle \cdot \rangle$ denotes averaging over all experimental realizations for fixed δ [16]. In the left panel of Fig. 2, we show the power spectra in the stable and unstable regimes, as well as at the critical point.

Besides a Fourier spectral decomposition, a study performed through a principal component analysis (PCA) offers a different way to link information compression to the atomic density distribution. PCA is a model-free approach which provides a lower-dimensional representation of a given data set by writing it as a linear combination of statistically uncorrelated normal modes (principal components) [28,29]. By carrying out PCA over the set of atomic-density maps, we can portray each individual frame $\Phi_i(x, y)$ as the sum of an average map and a linear combination of orthogonal modes $\mathcal{U}_m(x, y)$ [30],

$$\tilde{\Phi}_i(x, y) = \sum_{m=1}^{M} \lambda_{m,i} \mathcal{U}_m(x, y), \tag{2}$$

$$\langle \mathcal{U}_m, \mathcal{U}_\ell \rangle = \mathrm{Tr}(\mathcal{U}_m^\dagger \mathcal{U}_\ell) = \delta_{m\ell}. \tag{3}$$
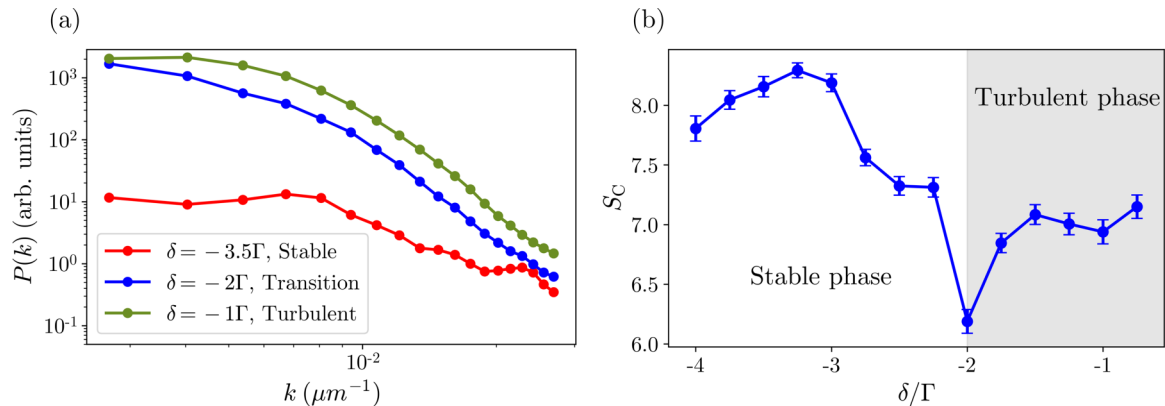
(a)

(b)

FIG. 2. (a) Radial component of the 2D average power spectrum in the stable and turbulent regimes and at criticality. In terms of magnitude, the turbulence phase is characterized by much larger fluctuations, when compared to the stable phase. (b) Configurational entropy computed from the spatial power spectrum as a function of the stress parameter δ. In the stable regime, the flatter power spectrum is reflected onto higher values of entropy. At $\delta = -2\Gamma$, the highly compact spectral distribution is at the origin of the entropy dip.

Above, the additional dependence on the stress parameter δ was omitted. The coefficients $\lambda_{m,j} \equiv \text{Tr}(\mathcal{U}_m^\dagger \tilde{\Phi}_j)$ are the projections onto the modes and we further define the mode variances as $\sigma_m^2 = \langle \lambda_{m,i}^2 \rangle$, denoting how much a given mode $\mathcal{U}_m$ contributes to representing the ensemble. The number of principal components is given by the number of degrees of freedom of each realization [here, it corresponds to the number of pixels in the charge-coupled device (CCD) camera], and we order them from the most to the least representative:

$$\sigma_1^2 \geqslant \sigma_2^2 \geqslant \cdots \geqslant \sigma_M^2 \geqslant 0, \quad \sum_{m=1}^M \sigma_m^2 = 1. \qquad (4)$$

The advantage of the analysis in terms of principal components is that, out of $M \sim 32\,000$ modes, only a few are of relevance to characterize the system dynamics. That is expressed by having $\sigma_m^2 \sim 0$ for $m > \overline{m}$, with $\overline{m} \ll M$ [see Fig. 3(b)], which lowers the dimensionality of the data set significantly. The first three PCA modes at three different values of the stress parameter—in the stable regime ($\delta = -3.5\Gamma$), at criticality ($\delta = -2\Gamma$), and in the turbulent regime ($\delta = -1\Gamma$)—are depicted in Fig. 3.

Contrary to Fourier modes, which are independent of the data set, principal components are retrieved directly from the data set itself: Fourier and PCA modes are representative of two different classes of basis decomposition, the former being an example of "universal" basis and, the latter, of "tailored" basis. The PCA decomposition allows us to highlight the similarities of the system dynamics along the whole range of δ. Within the same regime (stable or turbulent), density fluctuations are described by analogous sets of principal components. Far in the stable region, the majority of the fluctuation power, captured in the first mode, is due to oscillations of the total number of atoms. Conversely, a limited but larger set of modes is necessary to characterize the turbulent regime. This is a feature reminiscent of low-dimensional chaos [31–34].

In complete analogy with the configurational entropy, information entropy based on the principal component decomposition can then be defined from the modal variances as $S_{\text{PCA}} = -\sum_m \sigma_m^2 \log(\sigma_m^2)$. It follows that high data

compressibility descends from a small amount of oscillating global patterns whose linear combination is able to describe the main system dynamics.

IV. ENTROPY SIGNATURE AT CRITICALITY

We shall now focus our attention on the stress parameter dependence of S_C and S_{PCA}, interpreting the two curves in terms of spatial complexity and of the resulting modal distribution, i.e., the power spectrum and principal component variance. In the right-hand panel of Fig. 2, we observe that, as δ is brought from the stable to the turbulent region, the configurational entropy is reduced. In the stable regime, high-entropy values characterize the highly symmetric, spatially uniform, physical system. The power spectrum is essentially flat as a consequence of the fact that the stable regime is dominated by uncorrelated fluctuations (white noise). Conversely, in the turbulent phase, the power spectrum is dominated by long-wavelength modes, which, in the real space, witness the formation of randomly distributed large-scale coherent structures. In other words, local order implies low values of configurational entropy. Concerning S_{PCA}, as depicted in Fig. 3(c), we observe the opposite dependence on δ: Low-entropy values characterize the stable regime whereas high values are associated with the turbulent phase. These high values stem from the increased spatial complexity of the atomic cloud in the turbulent regime, where a larger number of principal components is necessary to represent the main system dynamics.

Remarkably, however, both S_{PCA} and S_C show a narrow dip at the turbulence edge, $\delta = \delta_c$, with $\delta_c \simeq -2\Gamma$, which we show to be related to the onset of the photon-bubble instability (check Appendixes A and B for details). As the system moves from one phase to another, it passes through an intermediate step where it reorganizes. The critical point is characterized by a divergence in the correlation length—analogous to critical opalescence [35,36]—in a configuration where both local and global order coexist. This highly structured state requires a low amount of information to be described, thus leading to a maximum in information compression. This quantity is not
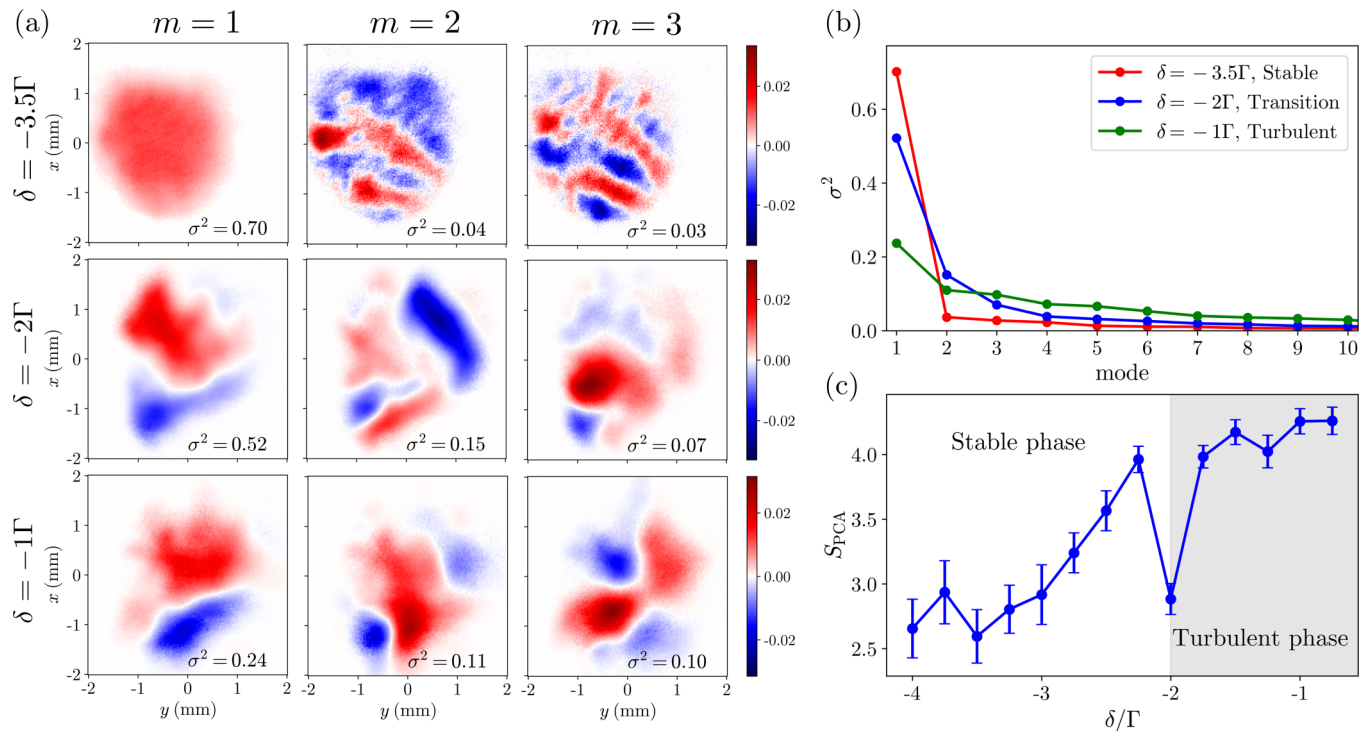
FIG. 3. (a) First three PCA modes in the stable regime (first row), at criticality (second row), and in the turbulent regime (third row); the color map represents density fluctuations. (b) Modal variance in the same regimes. (c) Entropy computed from the modal variance as a function of the detuning of the trapping lasers which drive the cold-atom cloud. Low values of entropy descend from a small amount of highly representative (high variance) modes which describe the system at a given δ.

only a measure of our knowledge of the system, but it is also a measure of complexity and order of a given spatial configuration, thus bearing information about the system physical properties.

Furthermore, theoretical and numerical studies have shown a configurational entropy dip at the onset of continuous
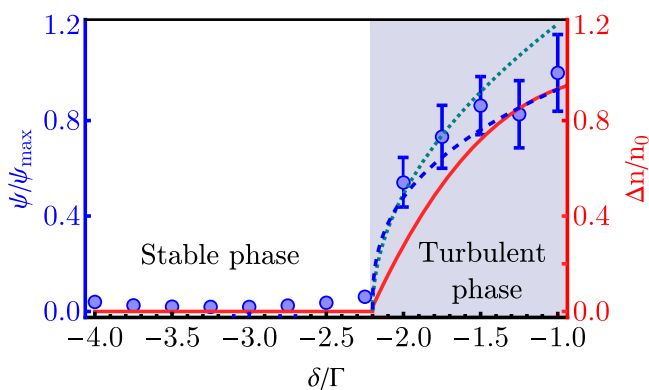

FIG. 4. Criticality and the onset of photon-bubble instability. The solid red line depicts the atomic depletion $\Delta n/n_0 \sim \delta_c + \delta$ as given by Eq. (B2) in Appendix B. The dots are the normalized fluctuation power resulting from the experimental data and the dashed green line is the universal critical function $(\delta_c + \delta)^{1/2}$, while the dashed blue line is the best fit $(\delta_c + \delta)^{0.372}$ discussed in the main text. This makes clear that the onset of the photon-bubble turbulence takes place in the interval $\delta \in [-2.25, -2]\Gamma$, compatible with the region in which information compression occurs.

equilibrium phase transitions [14,37]. Here, the same feature has been experimentally observed for an out-of-equilibrium phase transition, thus raising Shannon entropy as a good candidate to interpret critical phenomena in light of information theory.

The universal character of the phase transition can be put in evidence within the Ginzburg-Landau framework. If we define the total fluctuation power $\psi = \sum_{\mathbf{k}} P(\mathbf{k})$, the free energy can be written as

$$\mathcal{F}[\psi] = \mathcal{F}_0 + a(\delta_c - \delta)\psi^2 + \frac{b}{2}\psi^4, \qquad (5)$$

with $\mathcal{F}_0$ being the free energy deep in the stable phase, and a and b some positive constants. Minimization of Eq. (5) yields $\psi = [(a/b)(\delta - \delta_c)]^{1/2}$ for $\delta > \delta_c$ and $\psi = 0$ otherwise. In Fig. 4, we fit the experimental data to a test function of the form $\psi \sim |\delta - \delta_c|^\beta$, and observe that the critical parameter scales with the critical exponent $\beta^{(\text{expt.})} \simeq 0.372 \pm 0.003$. The experimental value of the exponent must be compared with that given by the mean-field approximation, $\beta^{(\text{MF})} = 1/2$, which deviates from $\beta^{(\text{expt.})}$ due to large fluctuations taking place at the critical point. Experimental measurements of β in other physical systems are in excellent agreement with that extracted from Fig. 4—see Ref. [38], where $\beta = 0.37 \pm 0.04$ was measured for the ferromagnetic transition in bulk lanthanum strontium manganese oxide (LSMO), and Refs. [39,40] where similar β values were reported for turbulent fluid and metal-insulator transitions. The latter suggests that the turbulent phase transition observed here is

well described in terms of the fluctuation power and falls into the universality class of second-order phase transitions.

V. CONCLUSIONS

Phase transitions in driven-dissipative systems are still far from being completely understood and theories lack experimental evidence. In this paper we have reported the observation of a maximum in information compression at the critical point of a far-from-equilibrium phase transition—which is the transition of a cold-atom cloud from a stable to a turbulent phase. Information compression at criticality is witnessed by a dip in information entropy which has been computed in two different ways by projecting the atomic density fluctuations on two distinct basis sets, the Fourier modes and the principal components. The two modal decompositions are associated in a complementary way to system complexity, one highlighting local order and the other the presence of fluctuating global patterns. Notably, information compression at criticality is independent of the representation used.

The experimental evidence we have provided shows that information entropy, built on either of two different modal decompositions, is capable of pinpointing the transition of a cold-atom cloud from stability to turbulence. If shared by a vast class of physical systems, this feature could raise information entropy to a fundamental quantity to develop a unifying phase transition theory. In the future, a more detailed analysis of the nonlinear stages of the instability based on the fluid description is required in order to quantitatively describe the width of the transition and therefore the validity of the diffusion approximation considered here. However, such a study is out of the scope of the present work and deserves further consideration in a separate publication.

APPENDIX A: THE DIFFUSION APPROXIMATION IN OPTICALLY THICK ATOMIC GASES

When the cooling laser is brought close to resonance, the cold atomic cloud behaves as an optically thick medium. As a consequence, light transport becomes diffusive and the laser intensity obeys the following diffusion equation [41–43],

$$\frac{\partial I}{\partial t} - \nabla \cdot (D\nabla I) = 0, \tag{A1}$$

where $D = \ell^2/\tau$ is the diffusion coefficient, with τ being the photon diffusion time, and ℓ the mean free path. The latter depends dynamically on the parameters of the atomic cloud as $\ell = 1/n\sigma_L$, where $n = n(\mathbf{r}, t)$ is the atomic density and

σ_L is the photon absorption cross section—which depends on the laser detuning $\delta = \omega_0 - \omega_a$ (here, ω_0 being the cooling laser frequency and ω_a the atomic transition frequency), as we will explicitly show below. To couple the dynamics of the light intensity I with that of the atomic density $n = n(\mathbf{r}, t)$ and velocity field $\mathbf{u} = \mathbf{u}(\mathbf{r}, t)$, we make use of a hydrodynamical model [44,45]

$$\frac{\partial n}{\partial t} + \nabla \cdot (n\mathbf{u}) = 0, \tag{A2}$$

$$\frac{\partial u}{\partial t} + (\mathbf{u} \cdot \nabla)\mathbf{u} = -\frac{\mathbf{F}}{m} - \nu\mathbf{u}, \tag{A3}$$

where m is the atomic mass, ν is the optical damping rate, and $\mathbf{F}$ is the collective force, given by [46]

$$\nabla \cdot \mathbf{F} = Qn. \tag{A4}$$

Here, $Q = \sigma_L(\sigma_R - \sigma_L)I/c$ is the effective charge, with σ_R denoting the absorption cross section for the rescattered photons [44,46]. Linearization of Eqs. (A1)–(A4) about the equilibrium quantities (n_0, I_0) in the form of plane waves (neglecting streaming here, $\mathbf{u}_0 = \mathbf{0}$),

$$n = n_0 + n_1 e^{(i\mathbf{k}\cdot\mathbf{r} - i\omega t)}, \quad I = I_0 + I_1 e^{(i\mathbf{k}\cdot\mathbf{r} - i\omega t)},$$

yields the following secular relation [24],

$$(\omega + i\nu)^2 = \omega_p^2 \left(1 + \frac{\omega_d}{i\omega - D_0 k^2}\right), \tag{A5}$$

where $D_0 = 1/(\tau n_0^2 \sigma_L^2)$ is the diffusion coefficient at equilibrium, $\omega_p = \sqrt{Qn_0/m}$ is the *plasma frequency* governing the timescale of the self-consistent forces due to multiple scattering, and $\omega_d = 2D_0\nabla^2 I_0/I_0$ is the diffusive photon-atom coupling. A dynamical instability (photon-bubble instability) takes place if $\gamma \equiv \text{Im}(\omega) > 0$, in which the growth rate is given by [24]

$$\gamma = -\left(\frac{\nu}{2} + \frac{\omega_d \omega_p^2}{\omega_p^2 + D_0^2 k^4}\right). \tag{A6}$$

Of course, Eq. (A6) and its implications in the quantitative estimates of the features of the phase transition, namely the width of transition and the correct amount of information depletion at criticality, are subject to the diffusion approximation considered in Eq. (A1). In any case, as we show below, this model is sufficient to describe the critical point of the transition, and therefore relate the observed information compression to the onset of photon-bubble instability. Future investigations would require the analysis of the functional dependence $D \sim n^{-2}$ employed in this work, to address the late (nonlinear) stages of the photon-bubble instability, and account for finite-size effects imposed by the trap. All those aspects, although pertinent, are technically complicated to address without sophisticated numerical simulations and are not critical in predicting the onset of the photon-bubble instability, as we detail below.

APPENDIX B: DENSITY DEPLETION AND CRITICALITY NEAR RESONANCE

Near resonance, $\delta \sim \Gamma$, the diffusive term $D_0 k^2$ dominates in Eqs. (A5) and (A6). At the onset of the instability, the

growth of a photon bubble pushes atoms away, leading to local atom depletion $n_0 \to n_0 - \Delta n$ occurring at the photon-bubble scale, i.e., $k^2 \sim \nabla^2 I_0 / I_0$ (notice that $\nabla^2 I_0 < 0$, and thus $\omega_d < 0$, for physically relevant situations—the intensity is larger at the center, as expected for a photon bubble forming at the center of the cloud). Under such circumstances, the instability threshold can be approximately expressed as

$$\frac{\omega_p^2 L^2}{\mathcal{D}_0} \simeq \frac{\nu}{2}, \tag{B1}$$

where we have defined the typical photon-bubble length $L = k^{-1}$ and the depleted diffusion coefficient, $\mathcal{D}_0 = D_0 n_0^2 / (n_0 - \Delta n)^2$. Equation (B1) thus yields the depletion as

$$\frac{\Delta n}{n_0} = 1 - \frac{1}{\omega_p L} \left(\frac{\nu \mathcal{D}_0}{2} \right)^{1/2}. \tag{B2}$$

In order to parametrize the depletion in terms of the experimentally accessible parameters, we consider a two-level atom theory, in which the relevant physical quantities read [45,46]

$$\sigma_L \simeq \frac{\sigma_0}{1 + I/I_{\text{sat}} + 4(\delta/\Gamma)^2}, \tag{B3}$$

$$Q \simeq \frac{\sigma_0^2 I^2}{c I_{\text{sat}}} \left(\frac{\Gamma}{2\delta} \right)^4, \tag{B4}$$

$$\nu \simeq -\frac{8\hbar k_0^2}{m} \frac{I/I_{\text{sat}}}{(1 + I/I_{\text{sat}})^2} \frac{\delta/\Gamma}{[1 + 4(\delta/\Gamma)^2]^2}. \tag{B5}$$

Here, $\sigma_0 = 3g\lambda_0^2/(2\pi)$ is the resonant cross section ($g = 3/7$ stands for the degeneracy parameter), $\lambda_0 = 780$ nm is the laser wavelength driving the ^{85}Rb D2 transition and $k_0 = 2\pi/\lambda_0$ is the associated wave vector, $\Gamma = 2\pi \times 5.89$ MHz is the transition linewidth, and $I_{\text{sat}} = 1.62$ mW/cm^{-2} is the saturation intensity [47]. Taking into account some additional experimental parameters, $L \simeq 4$ mm, $n_0 \simeq 3.7 \times 10^{10}$ cm^{-3}, and $I/I_{\text{sat}} \simeq 3.5$, and considering that in resonance we have $\tau \sim 8\Gamma^{-1}$ [48], we may plot the atomic depletion as a function of the detuning in Fig. 4. We can observe that the depletion becomes critical near $\delta \equiv \delta_c \sim -2\Gamma$, in very good agreement with the behavior of the fluctuation power discussed in the main text. It is nevertheless important to stress that although Δn has the same critical threshold as the fluctuation power—making therefore clear that the information compression observed in the main text is intimately related to the photon-bubble turbulence phenomenon—it is not the proper order parameter, since it scales as $(\delta_c + \delta)$. Alternatively, the fluctuation power is the correct order parameter describing the thermodynamics of the turbulent phase transition, as it falls in the universality class of the second-order phase transitions, with the critical scaling $(\delta_c + \delta)^{1/2}$. In any case, it is important to remark that despite the order of magnitude being correct, the precision on these estimations is limited by the uncertainties on the local values of the laser intensity and the number of atoms in the cloud, as well as by the effect of the finite laser linewidth which tends to smooth out the transition.

[1] H. H. Gibbs, Izaak Walton, Notes Queries **s4-XII**, 382 (1873).

[2] E. Jaynes, The minimum entropy production principle, Annu. Rev. Phys. Chem. **31**, 579 (1980).

[3] I. Prigogine, Dissipative structures, dynamics and entropy, Int. J. Quantum Chem. **9**, 443 (1975).

[4] I. Prigogine, Time, structure, and fluctuations, Science **201**, 777 (1978).

[5] J. M. Parrondo, J. M. Horowitz, and T. Sagawa, Thermodynamics of information, Nat. Phys. **11**, 131 (2015).

[6] V. DeGiorgio and M. O. Scully, Analogy between the laser threshold region and a second-order phase transition, Phys. Rev. A **2**, 1170 (1970).

[7] B. T. Walker, J. D. Rodrigues, H. S. Dhar, R. F. Oulton, F. Mintert, and R. A. Nyman, Non-stationary statistics and formation jitter in transient photon condensation, Nat. Commun. **11**, 1390 (2020).

[8] P. W. Egolf and K. Hutter, The mean field theories of magnetism and turbulence, Entropy **19**, 589 (2017).

[9] P. W. Egolf and K. Hutter, *Nonlinear, Nonlocal and Fractional Turbulence*, Graduate Studies in Mathematics (Springer, Berlin, 2020).

[10] H. Hinrichsen, Non-equilibrium phase transitions, Physica A **369**, 1 (2006).

[11] L. Brillouin, The negentropy principle of information, J. Appl. Phys. **24**, 1152 (1953).

[12] E. Jaynes, Predictive statistical mechanics, in *Frontiers of Nonequilibrium Statistical Physics*, edited by G. T. Moore and M. O. Scully, NATO Science Series B Vol. 135 (Springer, Berlin, 1986).

[13] A. F. Heavens, E. Sellentin, and A. H. Jaffe, Extreme data compression while searching for new physics, Mon. Not. R. Astron. Soc. **498**, 3440 (2020).

[14] D. Sowinski and M. Gleiser, Information dynamics at a phase transition, J. Stat. Phys. **167**, 1221 (2017).

[15] L. Landau and E. Lifshitz, *Statistical Physics* (Elsevier, Amsterdam, 2013), Vol. 5.

[16] R. Giampaoli, J. D. Rodrigues, J. A. Rodrigues, and J. T. Mendonça, Photon bubble turbulence in cold atom gases, Nat. Commun. **12**, 3240 (2021).

[17] M. Gaudesius, Y.-C. Zhang, T. Pohl, R. Kaiser, and G. Labeyrie, Three-dimensional simulations of spatiotemporal instabilities in a magneto-optical trap, Phys. Rev. A **105**, 013112 (2022).

[18] R. K. Niven, Minimization of a free-energy-like potential for non-equilibrium flow systems at steady state, Philos. Trans. R. Soc. B **365**, 1323 (2010).

[19] K. A. Takeuchi, M. Kuroda, H. Chaté, and M. Sano, Directed percolation criticality in turbulent liquid crystals, Phys. Rev. Lett. **99**, 234503 (2007).

[20] K. A. Takeuchi, Experimental approaches to universal out-of-equilibrium scaling laws: turbulent liquid crystal and other developments, J. Stat. Mech. (2014) P01006.

[21] E. Raab, M. Prentiss, A. Cable, S. Chu, and D. E. Pritchard, Trapping of neutral sodium atoms with radiation pressure, Phys. Rev. Lett. **59**, 2631 (1987).

[22] J. D. Rodrigues, J. A. Rodrigues, O. L. Moreira, H. Terças, and J. T. Mendonça, Equation of state of a laser-cooled gas, Phys. Rev. A **93**, 023404 (2016).

[23] J. Rodrigues, J. Rodrigues, A. Ferreira, and J. Mendonça, Collective processes in a large atomic laser cooling experiment, Opt. Quantum Electron. **48**, 169 (2016).

[24] J. Mendonça and R. Kaiser, Photon bubbles in ultracold matter, Phys. Rev. Lett. **108**, 033001 (2012).

[25] C. E. Shannon, The mathematical theory of communication, Bell Syst. Tech. J. **27**, 379 (1948); **27**, 623 (1948).

[26] R. V. Hartley, Transmission of information 1, Bell Syst. Tech. J. **7**, 535 (1928).

[27] M. Gleiser and N. Stamatopoulos, Entropic measure for localized energy configurations: Kinks, bounces, and bubbles, Phys. Lett. B **713**, 304 (2012).

[28] C. M. Bishop and N. M. Nasrabadi, *Pattern Recognition and Machine Learning* (Springer, Berlin, 2006).

[29] S. L. Brunton and J. N. Kutz, *Data-Driven Science and Engineering: Machine Learning, Dynamical Systems, and Control* (Cambridge University Press, Cambridge, UK, 2022).

[30] J. D. Rodrigues, R. Giampaoli, J. A. Rodrigues, A. V. Ferreira, H. Terças, and J. T. Mendonça, Quasi-static and dynamic photon bubbles in cold atom clouds, Atoms **10**, 45 (2022).

[31] A. Brandstäter, J. Swift, H. L. Swinney, A. Wolf, J. D. Farmer, E. Jen, and J. P. Crutchfield, Low-dimensional chaos in a hydrodynamic system, Phys. Rev. Lett. **51**, 1442(E) (1983).

[32] G. Hu, Y. Zhang, H. A. Cerdeira, and S. Chen, From low-dimensional synchronous chaos to high-dimensional desynchronous spatiotemporal chaos in coupled systems, Phys. Rev. Lett. **85**, 3377 (2000).

[33] E. Ott and T. M. Antonsen, Low dimensional behavior of large systems of globally coupled oscillators, Chaos **18**, 037113 (2008).

[34] R. Cestnik and A. Pikovsky, Hierarchy of exact low-dimensional reductions for populations of coupled oscillators, Phys. Rev. Lett. **128**, 054101 (2022).

[35] C. Walsh, P. Sémon, G. Sordi, and A.-M. S. Tremblay, Critical opalescence across the doping-driven Mott transition in optical lattices of ultracold atoms, Phys. Rev. B **99**, 165151 (2019).

[36] S. Kundu, T. Bar, R. K. Nayak, and B. Bansal, Critical slowing down at the abrupt Mott transition: When the first-order phase transition becomes zeroth order and looks like second order, Phys. Rev. Lett. **124**, 095703 (2020).

[37] M. Gleiser and D. Sowinski, Information-entropic signature of the critical point, Phys. Lett. B **747**, 125 (2015).

[38] K. Ghosh, C. J. Lobb, R. L. Greene, S. G. Karabashev, D. A. Shulyatev, A. A. Arsenov, and Y. Mukovskii, Critical phenomena in the double-exchange ferromagnet $La_{0.7}Sr_{0.3}MnO_3$, Phys. Rev. Lett. **81**, 4740 (1998).

[39] J. Sengers and J. Shanks, Experimental critical-exponent values for fluids, J. Stat. Phys. **137**, 857 (2009).

[40] A. Ionov, I. Shlimak, and M. Matveev, An experimental determination of the critical exponents at the metal-insulator transition, Solid State Commun. **47**, 763 (1983).

[41] A. Ishimaru, Scattering of waves from random continuum and turbulent media, in *Wave Propagation and Scattering in Random Media* (Academic, New York, 1978), Chap. 16.

[42] M. C. W. van Rossum and T. M. Nieuwenhuizen, Multiple scattering of classical waves: microscopy, mesoscopy, and diffusion, Rev. Mod. Phys. **71**, 313 (1999).

[43] H. Terças, J. T. Mendonça, and V. Guerra, Classical rotons in cold atomic traps, Phys. Rev. A **86**, 053630 (2012).

[44] T. Walker, D. Sesko, and C. Wieman, Collective behavior of optically trapped neutral atoms, Phys. Rev. Lett. **64**, 408 (1990).

[45] J. T. Mendonça, R. Kaiser, H. Terças, and J. Loureiro, Collective oscillations in ultracold atomic gas, Phys. Rev. A **78**, 013408 (2008).

[46] L. Pruvost, I. Serre, H. T. Duong, and J. Jortner, Expansion and cooling of a bright rubidium three-dimensional optical molasses, Phys. Rev. A **61**, 053408 (2000).

[47] G. Labeyrie, R. Kaiser, and D. Delande, Radiation trapping in a cold atomic gas, Appl. Phys. B **81**, 1001 (2005).

[48] G. Labeyrie, E. Vaujour, C. A. Müller, D. Delande, C. Miniatura, D. Wilkowski, and R. Kaiser, Slow diffusion of light in a cold atomic cloud, Phys. Rev. Lett. **91**, 223904 (2003).